

Published in final edited form as:

Cancer Biol Ther. 2009 November ; 8(21): 2042–2050.

Amplification of chromosomal segment 4q12 in non-small cell lung cancer

Alex H. Ramos^{1,2,3,†}, Amit Dutt^{1,2,†}, Craig Mermel^{1,2,3}, Sven Perner⁴, Jeonghee Cho¹, Christopher J. Lafargue⁵, Laura A. Johnson^{1,2}, Ann-Cathrin Stiedl⁴, Kumiko E. Tanaka^{1,2}, Adam J. Bass^{1,2}, Jordi Barretina^{1,2}, Barbara A. Weir^{1,2}, Rameen Beroukhi^{1,2}, Roman K. Thomas^{6,7}, John D. Minna^{8,9,10}, Lucian R. Chirieac^{3,11}, Neal I. Lindeman^{3,11}, Thomas Giordano¹², David G. Beer¹³, Patrick Wagner⁵, Ignacio I. Wistuba^{14,15}, Mark A. Rubin⁵, and Matthew Meyerson^{1,2,3,*}

¹Department of Medical Oncology and Center for Cancer Genome Discovery; Dana-Farber Cancer Institute; Boston, MA USA

²Cancer Program; Broad Institute of Harvard and MIT; Cambridge, MA USA

³Department of Pathology; Harvard Medical School; Boston, MA USA

⁴Department of Pathology; University Hospital of Tübingen; Tübingen, Germany

⁵Department of Pathology; Weill Medical College of Cornell University; New York, NY USA

⁶Max Planck Institute for Neurological Research with Klaus-Joachim-Zülch Laboratories of the Max-Planck Society and the Medical Faculty of the University of Cologne; Cologne, Germany

⁷Center for Integrated Oncology and Department for Internal Medicine; University of Cologne; Cologne, Germany

⁸Hamon Center for Therapeutic Oncology Research-Simmons Cancer Center; and Department of University of Texas Southwestern Medical Center; Dallas, TX USA

⁹Department of Internal Medicine; University of Texas Southwestern Medical Center; Dallas, TX USA

¹⁰Department of Pharmacology; University of Texas Southwestern Medical Center; Dallas, TX USA

¹¹Department of Pathology; Brigham and Women's Hospital; Boston, MA USA

¹²Department of Pathology; University of Michigan; Ann Arbor, MI USA

¹³Section of Thoracic Surgery; Department of Surgery; University of Michigan; Ann Arbor, MI USA

¹⁴Department of Epidemiology; The University of Texas M.D. Anderson Cancer Center; Houston, TX USA

¹⁵Department of Pathology; The University of Texas M.D. Anderson Cancer Center; Houston, TX USA

Abstract

© 2009 Landes Bioscience

*Correspondence to: Matthew Meyerson; Matthew_Meyerson@dfci.harvard.edu.

†These authors contributed equally to this work.

Supplementary materials can be found at: www.landesbioscience.com/supplement/RamosCBT8-21-Sup.pdf.

In cancer, proto-oncogenes are often altered by genomic amplification. Here we report recurrent focal amplifications of chromosomal segment 4q12 overlapping the proto-oncogenes *PDGFRA* and *KIT* in non-small cell lung cancer (NSCLC). Single nucleotide polymorphism (SNP) array and fluorescent in situ hybridization (FISH) analysis indicate that 4q12 is amplified in 3–7% of lung adenocarcinomas and 8–10% of lung squamous cell carcinomas. In addition, we demonstrate that the NSCLC cell line NCI-H1703 exhibits focal amplification of *PDGFRA* and is dependent on PDGFR α activity for cell growth. Treatment of NCI-H1703 cells with *PDGFRA*-specific shRNAs or with the PDGFR α /KIT small molecule inhibitors imatinib or sunitinib leads to cell growth inhibition. However, these observations do not extend to NSCLC cell lines with lower-amplitude and broader gains of chromosome 4q. Together these observations implicate *PDGFRA* and *KIT* as potential oncogenes in NSCLC, but further study is needed to define the specific characteristics of those tumors that could respond to PDGFR α /KIT inhibitors.

Keywords

NSCLC; lung cancer; *PDGFRA*; *KIT*; sunitinib; imatinib; amplification; 4q12

Introduction

In the United States, as well as worldwide, lung cancer is the leading cause of cancer mortality. The majority of lung cancer cases are non-small cell lung cancers (NSCLC), the most common forms of which are the two histological subtypes, adenocarcinoma and squamous cell carcinoma. Despite advances in systemic therapies and surgical techniques, 5-year survival rates for all types and stages of lung cancer remain low (16%).¹

Like other solid tumors, NSCLC cases are subject to large scale rearrangements leading to copy number gains and losses across the genome.^{2–4} Systematic analyses of copy number alterations in lung adenocarcinoma have identified genes such as *EGFR*, *MYC*, *MDM2*, *TERT*, *NKX2-1*, *PIK3CA* and *MET* to be selectively amplified.^{5–8} Other studies focusing on oncogenic point mutations have identified recurrent mutations leading to aberrant activation of *EGFR*, *KRAS*, *PIK3CA*, *ERBB2* and *BRAF* among other genes.^{9–12} Furthermore, inactivating point mutations and deletions in *TP53*, *STK11*, *NF1*, *CDKN2A* and *PTEN* have been reported.^{13–17} Most recently, mutations in several tyrosine kinase genes including *PDGFRA* and *KDR* have also been reported.¹⁵ Compared to lung adenocarcinoma, the range of genetic alterations in lung squamous cell carcinoma is less understood. Activating deletions in the extracellular domain of *EGFR* (*EGFRvIII* mutation) have been identified in 5% of lung squamous cell carcinoma samples examined.¹⁸ In addition, chromosome 3q amplifications have been found in 18% of lung squamous cell carcinoma samples.¹⁹ Nonetheless, despite these efforts to characterize the NSCLC genome, further work is needed to identify the complete spectrum of genetic lesions involved in NSCLC pathogenesis.

Importantly, a recent study using a proteomic approach to discover kinases activated in lung cancer identified phosphorylation of the receptor tyrosine kinase PDGFR α in 5% (8/150) of primary NSCLC cases and in the cell line NCI-H1703.²⁰ Treatment of NCI-H1703 cells with imatinib, an FDA-approved PDGFR α and KIT inhibitor, resulted in apoptotic cell death. Furthermore, while this manuscript was in review, an independent study demonstrated *PDGFRA* and *PDGFC* amplification and consequent PDGFR α activation in this cell line.²¹ In other tumors, aberrant activation of PDGFR α and KIT has been shown to play a tumorigenic role in gastrointestinal stromal tumors (GIST) and several brain tumor types.^{22,23} Constitutively activating point mutations in *PDGFRA* are found in 5% of GIST cases. Additionally, chromosomal region 4q12 harboring *PDGFRA* and *KIT* is often

amplified in glioblastoma multiforme (GBM) and other malignant brain tumors. Thus, there is evidence for a role for PDGFR α and KIT activation in NSCLC and other tumors, but the spectrum and impact of copy number alterations of these genes in NSCLC has not been characterized. We therefore sought to characterize *PDGFRA* in NSCLC using a combination of copy number analyses in primary samples and in vitro experiments in cell line models.

Results

Chromosomal segment 4q12 is recurrently amplified in non-small cell lung cancer

To characterize 4q12 copy number status in NSCLC, both previously published^{5,24,25} and unpublished Affymetrix 250K SNP array data for 733 NSCLC samples (628 primary samples, 105 cell lines) were evaluated for copy number aberrations (Fig. 1A; **Suppl. Table S1**).^{5,24–26} 4q12 amplifications overlapping the *PDGFRA/KIT* locus were observed in 31 (4.2%) NSCLC samples (Fig. 1B; **Suppl. Table S2**). The majority (93%; 29/31) of these amplifications were relatively focal events (<50% of the length of chromosome 4q) suggesting that selective amplification of target genes is occurring. The inferred copy number of the amplifications, normalized to a copy number of 2 for each sample, ranged from 2.5 to 10.2 copies (median = 2.8 copies); please note that these numbers are approximations that are both attenuated and non-integer for multiple reasons including stromal admixture, saturation of the SNP array at higher copy numbers, normalization to diploid normal control samples, and microarray signal measurement error.

The size of the focal amplifications ranged from 0.45 to 48.4 Mb (median = 7.55 Mb), respectively. Using the GISTIC (Genomic Identification of Significant Targets in Cancer) algorithm,²⁷ a 600 Kb region on 4q12 (54.76 to 55.36 Mb) was found to be significantly amplified. The sole genes within this region are *PDGFRA* and the closely related receptor tyrosine kinase *KIT*. Interestingly, our group has recently reported recurrent point mutations in *KDR*, a VEGFR family receptor tyrosine kinase located adjacent to *KIT*, as well as in *PDGFRA* and rarely in *KIT*.¹⁵ In our copy number data, *KDR* is often amplified with *PDGFRA* and *KIT* (28/31 samples) but it does not fall within the GISTIC region of statistical significance.

Comparing NSCLC subtypes, 3.5% (21/588) of adenocarcinomas and 8.7% (5/57) of squamous cell carcinomas harbored 4q12 amplifications, indicating that 4q12 is amplified at appreciable frequencies across both major NSCLC subtypes. No statistically significant correlations were observed between the presence of 4q12 amplification and available clinical parameters, including the histology, degree of histological differentiation, and stage at surgical resection of the tumors; and the age, gender, and reported ethnicity of the patients (**Suppl. Table S3**).

Most of the samples (26/29) with focal amplification at 4q12 had amplicons spanning both *PDGFRA* and *KIT* (Fig. 1B). However, three samples had amplicon breakpoints between *PDGFRA* and *KIT* and only amplify one of the two genes. Two primary adenocarcinoma samples, SM-11SU and SM-11U9, are *PDGFRA*^{WT}/*KIT*^{AMPLIFIED} while the lung squamous cell carcinoma cell line NCI-H1703 is *PDGFRA*^{AMPLIFIED}/*KIT*^{WT} (Suppl. Fig. S1). Importantly, the lung squamous cell carcinoma cell line NCI-H1703 has been shown to overexpress phosphorylated PDGFR α and to exhibit activated MAP kinase pathway signaling.²⁰ To identify any possible activating point mutations or insertion/deletions in NCI-H1703, the coding region of *PDGFRA* cDNA was sequenced but the only somatic alteration found was a G79D missense mutation listed in the dbSNP database (<http://www.ncbi.nlm.nih.gov/SNP/>) and unlikely to be activating (data not shown).

To validate our initial findings, we performed FISH in an independent set of 498 primary NSCLC tumor samples using a bacterial artificial chromosome (BAC) probe overlapping *PDGFRA* (Fig. 1C; Table 1). A BAC probe overlapping a non-amplified genomic region (4q21), as indicated by SNP array analysis, was used as a control. Of the 498 NSCLC samples evaluated, 39 (7.83%) were found to have amplification of the *PDGFRA* locus. Within subtypes, *PDGFRA* amplification was detected in 6.71% (21/313) of adenocarcinoma and 10.56% (9/161) of squamous cell carcinoma samples, closely mirroring the results ascertained by SNP array analysis (Table 1). Interestingly, two different amplification phenotypes were observed. Twenty-seven samples exhibited high-level amplification (CN > 10) of *PDGFRA* while 12 samples harbored lower levels of *PDGFRA* gain (CN 4–8).

To determine if samples with amplification of 4q12 also express PDGFR α or KIT, IHC was performed on 63 samples in TMAs in which 4q12 copy number status was known by FISH (**Suppl. Table S4**). We obtained high quality data for KIT staining, with clear membrane/cytoplasmic staining (Suppl. Fig. S2A). In total, 73% of samples were positive for KIT (46/63), with strong KIT staining (an IHC score of 3) seen in 6% (4/63) of cases. Of the four samples with strong KIT staining, one exhibited high-level 4q12 amplification, while three were diploid at 4q12. Overall, the intensity of KIT immunostaining was not correlated with 4q12 amplification status (Suppl. Fig. S2B). These results are consistent with a study by Holtkamp et al. showing frequent KIT expression independent of 4q12 amplification status in GBM samples.²⁸ We attempted anti-PDGFR α immunostaining on the same TMAs with multiple antibodies, but did not observe clear cytoplasmic/membranous staining that excluded the nuclei; we therefore have some concern that there may be non-specific nuclear immunoreactivity for the anti-PDGFR α antibodies used. Similar observations have been observed by others who have reported that anti-PDGFR α immunostaining is unreliable.²⁹ Observed non-nuclear IHC staining for PDGFR α is reported in **Supplementary Table S4**.

PDGFR α is essential for tumor cell survival in NCI-H1703 cells

Unregulated expression of oncogenes is necessary for tumor cell proliferation and viability. Given this dependency upon continued oncogenic signaling, termed oncogene addiction, tumor cells with genetically altered oncogenes can often be effectively treated with targeted agents.³⁰ Six cell lines harboring 4q12 copy number gain, whether broad or focal, were tested for PDGFR α expression (Suppl. Fig. S3A). Of these, only NCI-H1703 cells highly expressed PDGFR α . Notably, when compared against the five 4q12-amplified cell lines that did not express PDGFR α , the 4q12 amplicon in NCI-H1703 cells is considerably more focal and is present at much higher copy number (24.2 vs. maximum of 13.2 for other cell lines) as determined by quantitative PCR (Suppl. Fig. S3B), suggesting that 4q12 amplicon size and amplification level may play a role in predicting gene overexpression. In support of this, we failed to observe any strong IHC staining for PDGFR α or KIT in primary samples harboring low-level gains of 4q12 (**Suppl. Table S4**).

In order to demonstrate a role for *PDGFRA* in the survival of NSCLC cells with high-level focal 4q12 amplification, we tested a series of shRNA constructs in NCI-H1703 cells and control HCC15 cells without 4q12 amplification. Three out of five short hairpin RNAs significantly knocked down *PDGFRA* expression in NCI-H1703 cells (Fig. 2A). This knock down of *PDGFRA* inhibited cell survival and anchorage-independent growth in NCI-H1703 cells, but not in the HCC15 cells (Fig. 2B and C; Suppl. Fig. S4A and B). Together, these observations implicate *PDGFRA* as an essential gene in a subset of NSCLC samples; similar to other known oncogenes, such as *EGFR* and *FGFR2*, that can render tumor cells dependent upon their activation.^{31,32}

Effect of PDGFR α kinase inhibitors on cells with 4q12 amplification

We then investigated whether inhibition of PDGFR α kinase activity with small molecule inhibitors could be effective against lung cancer-derived cell lines with 4q12 amplification. To this end, we examined the effect of two small molecule tyrosine kinase inhibitors, imatinib and sunitinib, that are approved for the treatment of leukemia, GIST and advanced renal cell carcinoma.^{33–35} While imatinib specifically inhibits tyrosine kinase activity of Abl, KIT and PDGFR α ; sunitinib is a multi-targeted tyrosine kinase inhibitor of VEGFR-family receptors, PDGFR-family receptors, KIT, Ret, Flt3 and CSF-1R.^{36,37} Treatment with imatinib or sunitinib resulted in a marked decrease of cell survival in NCI-H1703 cells (IC₅₀ of 20 nM and 74 nM) but not the other cell lines tested including five with 4q12 gain (Fig. 3A and B; Suppl. Fig. S5A and B) and also led to decreased colony formation in NCI-H1703 cells (Suppl. Fig. S6A and B). Consistent with this in vitro effect, treatment with 2 μ M imatinib or sunitinib for 40 minutes at 37°C inhibited the constitutive phosphorylation of PDGFR α in NCI-H1703 cells (Fig. 3C).

Discussion

We have identified recurrent focal amplifications of chromosomal region 4q12 in NSCLC. Systematic statistical analysis suggests that the proto-oncogenes *PDGFRA* and *KIT* are the target of these copy number gains. High-level focal amplifications of 4q12 have been widely described in GBM and are observed in 10–15% of cases.³⁸ Our results indicate 3–10% frequencies of 4q12 amplification in both lung adenocarcinoma and lung squamous cell carcinoma. A genome wide copy number analysis by our group in a diverse dataset of 13 different tissue types detects recurrent 4q12 amplification only in glioma and NSCLC tumors (Beroukhi, Mermel et al. in preparation), suggesting that *PDGFRA* and *KIT* amplification may play a tumorigenic role in only a few cancer types.

In brain tumors, *PDGFRA* and *KIT* are often amplified together, however expression of the protein products is independent of gene amplification status.^{28,39,40} We report comparable findings in both primary and cell line NSCLC samples. Of the six cell lines with 4q12 amplification that were tested, only NCI-H1703 cells expressed and activated PDGFR α . It is uncertain what determinants are driving PDGFR α overexpression and activation in the context of 4q12 amplification. We have recently identified *PDGFRA* and *KDR* as significantly mutated genes in lung adenocarcinoma however all 14 samples (n = 188) with *PDGFRA* or *KDR* mutation did not harbor 4q12 amplification suggesting that mutation and amplification are mutually exclusive events.¹⁵ Recently, McDermott and colleagues have shown that endogenous co-amplification and overexpression of *PDGFC*, which encodes a ligand of PDGFR α , in NCI-H1703 cells is also involved in this cell line's oncogenic signaling.²¹ We confirm *PDGFC* amplification in NCI-H1703 cells but fail to find focal *PDGFRA* and *PDGFC* co-amplification in our dataset of 628 primary samples (data not shown). It is likely that 4q12 amplification alone is not sufficient for PDGFR α activation and additional factors may be required for PDGFR α -mediated signaling. Additional experiments will be necessary to characterize the complete spectrum of genetic alterations and protein interactions underlying PDGFR α activation in the context of 4q12 amplification.

In this study we also demonstrate that the lung cancer cell line NCI-H1703 focally amplifies *PDGFRA* and is dependent on PDGFR α signaling for cell growth. Treatment of NCI-H1703 cells with *PDGFRA*-specific shRNAs and the small molecule inhibitors imatinib or sunitinib leads to cell death suggesting that targeted therapy of PDGFR α may be clinically feasible in a molecularly defined subset of NSCLC patients. However, our FISH and IHC findings suggest that high-level 4q12 amplification alone will not sufficiently predict response to imatinib or sunitinib. Moreover, since the co-amplification of *PDGFRA* and *PDGFC* seen in NCI-H1703 cells is a rare event, further work is needed to identify additional NSCLC

models that more accurately mimic the aberrant PDGFR α signaling observed in primary samples. Future genomic and functional work in such models will greatly aid in deriving more robust biomarkers of imatinib and sunitinib sensitivity. In addition, the role of *KIT* in NSCLC tumorigenesis is unclear due to the lack of lung cancer cell line models that display *KIT* expression concomitant with endogenous *KIT* amplification in which to perform functional testing.

The advent of targeted cancer therapeutics emphasizes the significance of identifying genetic alterations that lead to oncogene dependency in tumors. Notably, discovery of tumorigenic NSCLC somatic alterations in proto-oncogenes with existing targeted therapeutic approaches in other cancer types could provide opportunities for immediate adoption of clinically approved treatments. In particular, a subset of NSCLC patients with high-level focal amplifications of 4q12 present an opportunity for successful targeted therapy with sunitinib, a compound that is FDA approved for several other cancer types. Interestingly, a phase II clinical trial of sunitinib in previously treated NSCLC patients demonstrated an objective response rate of 11% (7/63 patients).⁴¹ It remains to be seen whether NSCLC patients responsive to sunitinib harbor 4q12 amplification and aberrant PDGFR α /*KIT* activation.

In conclusion, our results identify chromosomal segment 4q12 as a region selected for amplification in NSCLC. Importantly, aberrant activation of PDGFR α and *KIT* in NSCLC presents potentially attractive prospects for successful targeted therapy with clinically approved kinase inhibitors. Our data indicate that amplification alone will not predict sensitivity to imatinib or sunitinib. It is possible that other genetic alterations such as small insertion/deletions and translocations could be involved in gene activation. Further work is needed to fully characterize the role of PDGFR α and *KIT* in NSCLC biology.

Materials and Methods

NSCLC primary samples and cell lines

For SNP array experiments, genomic DNA was extracted from 25 fresh frozen primary tumors and 5 cell lines. Primary samples were collected from six different sites: Memorial-Sloan Kettering Cancer Center (2 tumors), University of Michigan (1 tumor), Washington University in St. Louis (3 tumors), Dana-Farber Cancer Institute/The Broad Institute (8 tumors), Brigham and Women's Hospital tissue bank (4 tumors), and from the University Health Network in Toronto (7 tumors). Five cell lines were obtained from ATCC. Processed SNP array data and raw cel files are publicly available in the Gene Expression Omnibus (GEO) repository (GEO accession number GSE17429). Additionally, raw Affymetrix 250K SNP array data from 556 primary adenocarcinomas as published in Weir et al. (<http://www.broadinstitute.org/tsp/>), 79 NSCLC cell lines as published in Sos et al. (GEO accession number GSE17247), 47 primary squamous cell carcinomas as published in Bass et al. and 21 NSCLC cell lines from the NCI caBIG database were utilized (https://cabig.nci.nih.gov/caArray_GSKdata/).^{5,24–26} Histological subtype for all cases was determined by the original pathologist at tumor resection, confirmed by a review group led by Dr. William Travis for the 554 primary adenocarcinomas described by Weir et al.⁵

For FISH and IHC experiments, tissue microarrays (TMAs) were provided by L.R.C., N.I.L., T.G., and I.I.W. Histology was confirmed by S.P. prior to FISH and IHC evaluation. In total, 15 TMAs comprising 901 cases were analyzed with I-FISH. 498 of these cases had a FISH amplification status that was assessable (403 cases either showed no tumor on the tissue cores or had insufficient hybridization).

SNP array experiments and analysis

SNP array experiments were performed on 733 NSCLC tumor and cell line samples as described in Weir et al.⁵ Data was analyzed using GISTIC as described in Beroukhi et al.²⁷ A description of our analysis using the GenePattern software package is provided in the Supplementary Materials under the heading, "Description of 250K SNP Array Analysis". Briefly, genomic DNA was genotyped using the Sty I chip of the 500K Human Mapping Array set (Affymetrix Inc.) at the Broad Institute. Raw probe intensities were processed using modules in GenePattern; copy number was computed by dividing the intensity of each probeset by the mean value of that probeset in the five closest normals by Euclidean distance (see Beroukhi et al.). Normalized data was segmented with GenePattern modules based on the GLAD algorithm. G-scores derived from GISTIC were obtained for each SNP probe across chromosome 4. Only amplifications exceeding log₂ ratio of 0.3 were included. G-scores were compared against a null model generated by random permutations to determine a false discovery rate (q-value). Peaks with q-values below 0.25 were considered significant. Both the peak region determined by minimal common overlap (chr4:54781155–54868471, probes 57234:57238) and the wide peak determined by a leave-one-out approach (chr4:54758116–55357275, probes 57231:57300) are reported (q-value = 0.08).

Dual-color interphase fluorescent in-situ hybridization on tissue microarrays (I-FISH on TMAs)

To assess for *PDGFRA* amplification, probe spanning *PDGFRA* (chr4q12, 99.3 kb) and a reference probe spanning a stable region identified by SNP data in NSCLC (chr4q22.3–q23, 193 kb) were used. For the *PDGFRA* target probe, the Biotin-14-dCTP labeled BAC clone CTD-2054G11 (conjugated to produce a red signal) was applied. For the reference probe, the Digoxigenin-11-dUTP labeled BAC clone RP11-799A12 (conjugated to produce a green signal) was applied. Correct chromosomal probe localization was confirmed on normal lymphocyte metaphase preparations. BAC clones were obtained from the BACPAC Resource Center, Children's Hospital Oakland Research Institute (CHORI) (Oakland, CA) and Invitrogen (Carlsbad, CA). Tissue hybridization, washing and color detection were performed as described previously.⁴² *PDGFRA* amplification by FISH was assessed in 498 samples (represented by 1442 TMA cores). At least one TMA core could be evaluated per case. The samples were analyzed under a 60x oil immersion objective using an Olympus BX-511 fluorescence microscope, a CCD (charge-coupled device) camera and the CytoVision FISH imaging and capturing software (Applied Imaging, San Jose, CA). Semi-quantitative evaluation of the tests was independently performed by three evaluators (A.R., S.P., and L.A.J.). For each case, we attempted to analyze at least 100 nuclei.

Immunohistochemistry

Immunohistochemistry for PDGFR α and KIT (CD117) was performed on 63 cases for which *PDGFRA* amplification status was known. Antibodies used for immunohistochemistry were anti-PDGFR α monoclonal antibody (1:50; clone: SPM473, Zytomed Systems), and anti-KIT polyclonal antibody (1:200; Dako Denmark A/S). Immunohistochemistry was performed as previously described.⁴³ At least one tissue microarray core was assessable per case. Each core was semi-quantitatively evaluated and scored for non-nuclear staining of PDGFR α and KIT. For KIT staining, cores were scored 0, 1, 2 and 3 according to the following criteria: 0, no staining; 1, weak staining in <50% of tumor cells; 2, moderate staining in >50% of tumor cells; and 3, strong staining in >90% of tumor cells. For PDGFR α staining, cores were scored 0, 1 and 2 according to the following criteria: 0, no staining; 1, weak staining in <50% of tumor cells; 2, strong staining in >50% of tumor cells. Mean IHC scores were used for cases in which multiple cores were assessable. Non-integer mean IHC score values were rounded to the nearest integer value.

Cell culture and reagents

The NSCLC cell lines, NCI-H1703 and HCC15 were obtained from ATCC (Manassas, Virginia, United States) and DSMZ (Braunschweig, Germany), respectively. Cells were maintained in RPMI 1640 complete media supplemented with 10% calf serum (Gibco/Invitrogen, Carlsbad, California, United States) and penicillin/streptomycin (Gibco/Invitrogen). Unless otherwise noted, cells were placed in media containing 0.5% calf serum 24 h prior to 100 ng/mL PDGF (#9909, Cell Signaling Technologies, Danvers, MA, United States) stimulation for 20 minutes at 37°C. Imatinib and Sunitinib were purchased from LC Laboratories (Woburn, Massachusetts, United States) and diluted in DMSO to the indicated concentrations.

shRNA mediated *PDGFRA* knockdown

shRNA vectors targeted against *PDGFRA* and *GFP* were obtained from TRC (The RNAi Consortium). The target sequences of the *PDGFRA* shRNA constructs are:

PDGFRA#1 (TRCN0000001422): 5'-CCC AAC TTT CTT ATC CAA CTT-3'.

PDGFRA#2 (TRCN0000001423): 5'-CCA GCC TCA TAT AAG AAG AAA-3'.

PDGFRA#3 (TRCN0000001424): 5'-CCA GCT TTC ATT ACC CTC TAT-3'.

PDGFRA#4 (TRCN0000001425): 5'-CGG TGA AAG ACA GTG GAG ATT-3'.

PDGFRA#5 (TRCN0000001426): 5'-CAA TGG ACT TAC CCT GGA GAA-3'.

The sequence targeted by the *GFP* shRNA is 5'-GCA AGC TGA CCC TGA AGT TCA T-3'. Lentiviruses were made by transfection of 293T packaging cells with these constructs using a three plasmid system as previously described.⁴⁴ Target cells were incubated with lentiviruses for 6 hours in the presence of 8 µg/ml polybrene and left in fresh media. Two days after infection, puromycin (2 µg/ml for NCI-H1703 and HCC15) was added. Cells were grown in the presence of puromycin for four days. Fifty micrograms of total cell lysates prepared from the puromycin selected cell lines was analyzed by western blotting using anti-PDGFR α monoclonal antibody (#sc-31166, Santa Cruz Biotechnology), anti-phospho-PDGFR α monoclonal antibody (#sc-12910, Santa Cruz Biotechnology), and anti-Actin monoclonal antibody (#sc-1615, Santa Cruz Biotechnology).

Cell survival assays with tumor cell lines expressing sh*PDGFRA* and sh*GFP* constructs

800 cells for each tumor cell line expressing shRNAs targeting *PDGFRA* or *GFP* along with uninfected cells were seeded in 6 wells on a 96 well plate. Cell viability was determined at 24 hour time points for 4 consecutive days using the WST-1 assay (Roche Applied Science). The percentage of cell viability is plotted for each cell line of readings obtained on Day 3 relative to Day 1.

Soft agar anchorage-independent growth assay with tumor cell lines expressing sh*PDGFRA* and sh*GFP* constructs

NCI-H1703 and HCC15 cells expressing sh*PDGFRA* and sh*GFP* were suspended in a top layer of RPMI1640 containing 10% calf serum and 0.4% Select agar (Gibco/Invitrogen, Carlsbad, California, United States) and plated on a bottom layer of RPMI1640 containing 10% calf serum and 0.5% Select agar. Imatinib or sunitinib were added as described to the top agar. After 3 weeks incubation for HCC15 cells and 5 weeks for NCI-H1703 cells, colonies were counted in triplicate. IC₅₀s were determined by nonlinear regression using Prism 5 software (GraphPad Software).

Cytotoxicity assays

Lung cancer cell lines were treated with imatinib or sunitinib one day after plating and cell survival was assessed 4 days later using the WST-1 assay (Roche Applied Science). Each data point represents the median of six replicate wells for each tumor cell line and inhibitor concentration. IC₅₀s were determined by nonlinear regression using the Prism Graphpad software.

Immunoblotting

Cells were lysed in a buffer containing 50 mM Tris-HCl (pH 7.4), 150 mM NaCl, 2.5 mM EDTA, 1% Triton X-100 and 0.25% IPEGAL. Protease inhibitors (Roche Applied Science) and phosphatase inhibitors (Calbiochem) were added prior to use. Samples were normalized for total protein content. Lysates were boiled in sample buffer, separated by SDS-PAGE on 8% polyacrylamide gels, transferred to PVDF membrane, and probed as described. Antibodies used for immunoblotting were: anti-PDGFR α monoclonal antibody (# sc-31166, Santa Cruz Biotechnology), anti-phospho-PDGFR α monoclonal antibody (# sc-12910, Santa Cruz Biotechnology), and anti-Actin monoclonal antibody (# sc-1615, Santa Cruz Biotechnology).

Quantitative real-time PCR

Relative gene copy number of *PDGFRA* was determined by quantitative real-time PCR as previously described.² Primer sequences used were:

PDGFRA 5': 5'-GTG GGA TAC TGA ATC TGG AAG G-3'.

PDGFRA 3': 5'-CGT GTT GGA GGT GTT AGC TGT A-3'.

LINE-1 5': 5'-AAA GCC GCT CAA CTA CAT GG-3'.

LINE-1 3': 5'-TGC TTT GAA TGC GTC CCA GA-3'.

PDGFRA transcript levels were determined by quantitative reverse transcriptase PCR using the $\Delta\Delta$ Ct method. Actin and the cell line LN-382 (known to express PDGFR α)⁴⁵ were used as controls. Primer sequences used were:

PDGFRA 5': 5'-GGC ACG CAT GCG TGT GGA CTC AG-3'.

PDGFRA 3': 5'-GTC TAT GCC GAT GTC ATC CAT-3'.

ACTIN 5': 5'-ACC AAC TGG GAC GAT ATG GAG AAG A-3'.

ACTIN 3': 5'-TAC GAC CAG AGG CAT ACA GGG ACA A-3'.

Supplementary Material

Refer to Web version on PubMed Central for supplementary material.

Acknowledgments

We thank Shantanu Banerji for critical reading of the manuscript and Christopher A. French for providing microscopy support. A.D. is supported by the Swiss National Science Foundation Fellowship #PBZHB-106297. This work was supported by National Cancer Institute grants 5R01CA109038 and 5P20CA90578 (M.M.).

References

1. Jemal A, Siegel R, Ward E, Hao Y, Xu J, Murray T, Thun MJ. Cancer statistics, 2008. *CA Cancer J Clin* 2008;58:71–96. [PubMed: 18287387]
2. Weir B, Zhao X, Meyerson M. Somatic alterations in the human cancer genome. *Cancer Cell* 2004;6:433–438. [PubMed: 15542426]

3. Tonon G, Brennan C, Protopopov A, Maulik G, Feng B, Zhang Y, et al. Common and contrasting genomic profiles among the major human lung cancer subtypes. *Cold Spring Harb Symp Quant Biol* 2005;70:11–24. [PubMed: 16869734]
4. Lockwood WW, Chari R, Coe BP, Girard L, Macaulay C, Lam S, et al. DNA amplification is a ubiquitous mechanism of oncogene activation in lung and other cancers. *Oncogene* 2008;27:4615–4624. [PubMed: 18391978]
5. Weir BA, Woo MS, Getz G, Perner S, Ding L, Beroukhi R, et al. Characterizing the cancer genome in lung adenocarcinoma. *Nature* 2007;450:893–898. [PubMed: 17982442]
6. Kwei KA, Kim YH, Girard L, Kao J, Pacyna-Gengelbach M, Salari K, et al. Genomic profiling identifies TITF1 as a lineage-specific oncogene amplified in lung cancer. *Oncogene* 2008;27:3635–3640. [PubMed: 18212743]
7. Yamamoto H, Shigematsu H, Nomura M, Lockwood WW, Sato M, Okumura N, et al. PIK3CA mutations and copy number gains in human lung cancers. *Cancer Res* 2008;68:6913–6921. [PubMed: 18757405]
8. Engelman JA, Zejnullahu K, Mitsudomi T, Song Y, Hyland C, Park JO, et al. MET amplification leads to gefitinib resistance in lung cancer by activating ERBB3 signaling. *Science* 2007;316:1039–1043. [PubMed: 17463250]
9. Davies H, Hunter C, Smith R, Stephens P, Greenman C, Bignell G, et al. Somatic mutations of the protein kinase gene family in human lung cancer. *Cancer Res* 2005;65:7591–7595. [PubMed: 16140923]
10. Samuels Y, Wang Z, Bardelli A, Silliman N, Ptak J, Szabo S, et al. High frequency of mutations of the PIK3CA gene in human cancers. *Science* 2004;304:554. [PubMed: 15016963]
11. Stephens P, Hunter C, Bignell G, Edkins S, Davies H, Teague J, et al. Lung cancer: intragenic ERBB2 kinase mutations in tumours. *Nature* 2004;431:525–526. [PubMed: 15457249]
12. Naoki K, Chen TH, Richards WG, Sugarbaker DJ, Meyerson M. Missense mutations of the BRAF gene in human lung adenocarcinoma. *Cancer Res* 2002;62:7001–7003. [PubMed: 12460919]
13. Takahashi T, Nau MM, Chiba I, Birrer MJ, Rosenberg RK, Vinocour M, et al. p53: a frequent target for genetic abnormalities in lung cancer. *Science* 1989;246:491–494. [PubMed: 2554494]
14. Sanchez-Cespedes M, Parrella P, Esteller M, Nomoto S, Trink B, Engles JM, et al. Inactivation of LKB1/STK11 is a common event in adenocarcinomas of the lung. *Cancer Res* 2002;62:3659–3662. [PubMed: 12097271]
15. Ding L, Getz G, Wheeler DA, Mardis ER, McLellan MD, Cibulskis K, et al. Somatic mutations affect key pathways in lung adenocarcinoma. *Nature* 2008;455:1069–1075. [PubMed: 18948947]
16. Packenham JP, Taylor JA, White CM, Anna CH, Barrett JC, Devereux TR. Homozygous deletions at chromosome 9p21 and mutation analysis of p16 and p15 in microdissected primary non-small cell lung cancers. *Clin Cancer Res* 1995;1:687–690. [PubMed: 9816033]
17. Forgacs E, Biesterveld EJ, Sekido Y, Fong K, Muneer S, Wistuba II, et al. Mutation analysis of the PTEN/MMAC1 gene in lung cancer. *Oncogene* 1998;17:1557–1565. [PubMed: 9794233]
18. Ji H, Zhao X, Yuza Y, Shimamura T, Li D, Protopopov A, et al. Epidermal growth factor receptor variant III mutations in lung tumorigenesis and sensitivity to tyrosine kinase inhibitors. *Proc Natl Acad Sci USA* 2006;103:7817–7822. [PubMed: 16672372]
19. Okudela K, Suzuki M, Kageyama S, Bunai T, Nagura K, Igarashi H, et al. PIK3CA mutation and amplification in human lung cancer. *Pathol Int* 2007;57:664–671. [PubMed: 17803655]
20. Rikova K, Guo A, Zeng Q, Possemato A, Yu J, Haack H, et al. Global survey of phosphotyrosine signaling identifies oncogenic kinases in lung cancer. *Cell* 2007;131:1190–1203. [PubMed: 18083107]
21. McDermott U, Ames RY, Iafrate AJ, Maheswaran S, Stubbs H, Greninger P, et al. Ligand-dependent platelet-derived growth factor receptor (PDGFR)-alpha activation sensitizes rare lung cancer and sarcoma cells to PDGFR kinase inhibitors. *Cancer Res* 2009;69:3937–3946. [PubMed: 19366796]
22. Hirota S, Ohashi A, Nishida T, Isozaki K, Kinoshita K, Shinomura Y, Kitamura Y. Gain-of-function mutations of platelet-derived growth factor receptor alpha gene in gastrointestinal stromal tumors. *Gastroenterology* 2003;125:660–667. [PubMed: 12949711]

23. Fleming TP, Saxena A, Clark WC, Robertson JT, Oldfield EH, Aaronson SA, Ali IU. Amplification and/or overexpression of platelet-derived growth factor. *Cancer Res* 1992;52:4550–4553. [PubMed: 1322795]
24. GlaxoSmithKline. GSK Cancer Cell Line Genomic Profiling Data. 2008
25. Bass A, Watanabe H, Yu S, et al. SOX2 is an amplified lineage-survival oncogene in lung and esophageal squamous cell carcinoma. *Nat Genet* in review.
26. Sos ML, Michel K, Zander T, Weiss J, Frommolt P, Peifer M, et al. Predicting drug susceptibility of non-small cell lung cancers based on genetic lesions. *J Clin Invest* 2009;119:1727–1740. [PubMed: 19451690]
27. Beroukhi R, Getz G, Nghiemphu L, Barretina J, Hsueh T, Linhart D, et al. Assessing the significance of chromosomal aberrations in cancer: methodology and application to glioma. *Proc Natl Acad Sci USA* 2007;104:20007–20012. [PubMed: 18077431]
28. Holtkamp N, Ziegenhagen N, Malzer E, Hartmann C, Giese A, von Deimling A. Characterization of the amplicon on chromosomal segment 4q12 in glioblastoma multiforme. *Neuro Oncol* 2007;9:291–297. [PubMed: 17504929]
29. Wetli SC, Leuschner I, Harms D, Ruffe A, Foerster A, Bihl M, et al. KIT, PDGFRalpha and EGFR analysis in nephroblastoma. *Virchows Arch* 2008;452:637–650. [PubMed: 18478259]
30. Sharma SV, Settleman J. Oncogene addiction: setting the stage for molecularly targeted cancer therapy. *Genes Dev* 2007;21:3214–3231. [PubMed: 18079171]
31. Greulich H, Chen TH, Feng W, Janne PA, Alvarez JV, Zappaterra M, et al. Oncogenic transformation by inhibitor-sensitive and -resistant EGFR mutants. *PLoS Med* 2005;2:313.
32. Dutt A, Salvesen HB, Chen TH, Ramos AH, Onofrio RC, Hatton C, et al. Drug-sensitive FGFR2 mutations in endometrial carcinoma. *Proc Natl Acad Sci USA* 2008;105:8713–8717. [PubMed: 18552176]
33. Wardelmann E, Merkelbach-Bruse S, Pauls K, Thomas N, Schildhaus HU, Heinicke T, et al. Polyclonal evolution of multiple secondary KIT mutations in gastrointestinal stromal tumors under treatment with imatinib mesylate. *Clin Cancer Res* 2006;12:1743–1749. [PubMed: 16551858]
34. van Oosterom AT, Judson I, Verweij J, Stroobants S, Donato di Paola E, Dimitrijevic S, et al. Safety and efficacy of imatinib (STI571) in metastatic gastrointestinal stromal tumours: a phase I study. *Lancet* 2001;358:1421–1423. [PubMed: 11705489]
35. Motzer RJ, Hutson TE, Tomczak P, Michaelson MD, Bukowski RM, Rixe O, et al. Sunitinib versus interferon alfa in metastatic renal-cell carcinoma. *N Engl J Med* 2007;356:115–124. [PubMed: 17215529]
36. Christensen JG. A preclinical review of sunitinib, a multitargeted receptor tyrosine kinase inhibitor with anti-angiogenic and antitumour activities. *Ann Oncol* 2007;18:3–10.
37. Karaman MW, Herrgard S, Treiber DK, Gallant P, Atteridge CE, Campbell BT, et al. A quantitative analysis of kinase inhibitor selectivity. *Nat Biotechnol* 2008;26:127–132. [PubMed: 18183025]
38. Comprehensive genomic characterization defines human glioblastoma genes and core pathways. *Nature* 2008;455:1061–1068. [PubMed: 18772890]
39. Joensuu H, Pupa M, Sihto H, Tynninen O, Nupponen NN. Amplification of genes encoding KIT, PDGFRalpha and VEGFR2 receptor tyrosine kinases is frequent in glioblastoma multiforme. *J Pathol* 2005;207:224–231. [PubMed: 16021678]
40. Pupa M, Tynninen O, Sihto H, Blom T, Maenpaa H, Isola J, et al. Amplification of KIT, PDGFRA, VEGFR2 and EGFR in gliomas. *Mol Cancer Res* 2006;4:927–934. [PubMed: 17189383]
41. Socinski MA, Novello S, Brahmer JR, Rosell R, Sanchez JM, Belani CP, et al. Multicenter, phase II trial of sunitinib in previously treated, advanced non-small-cell lung cancer. *J Clin Oncol* 2008;26:650–656. [PubMed: 18235126]
42. Perner S, Wagner P, Soltermann A, Lafargue C, Tischler V, Weir B, et al. TTF1 expression in non-small cell lung carcinoma: association with TTF1 gene amplification and improved survival. *J Pathol*. 2008

43. Tomlins SA, Rhodes DR, Yu J, Varambally S, Mehra R, Perner S, et al. The role of SPINK1 in ETS rearrangement-negative prostate cancers. *Cancer Cell* 2008;13:519–528. [PubMed: 18538735]
44. Moffat J, Grueneberg DA, Yang X, Kim SY, Kloepper AM, Hinkle G, et al. A lentiviral RNAi library for human and mouse genes applied to an arrayed viral high-content screen. *Cell* 2006;124:1283–1298. [PubMed: 16564017]
45. Giannini C, Sarkaria JN, Saito A, Uhm JH, Galanis E, Carlson BL, et al. Patient tumor EGFR and PDGFRA gene amplifications retained in an invasive intracranial xenograft model of glioblastoma multiforme. *Neuro Oncol* 2005;7:164–176. [PubMed: 15831234]

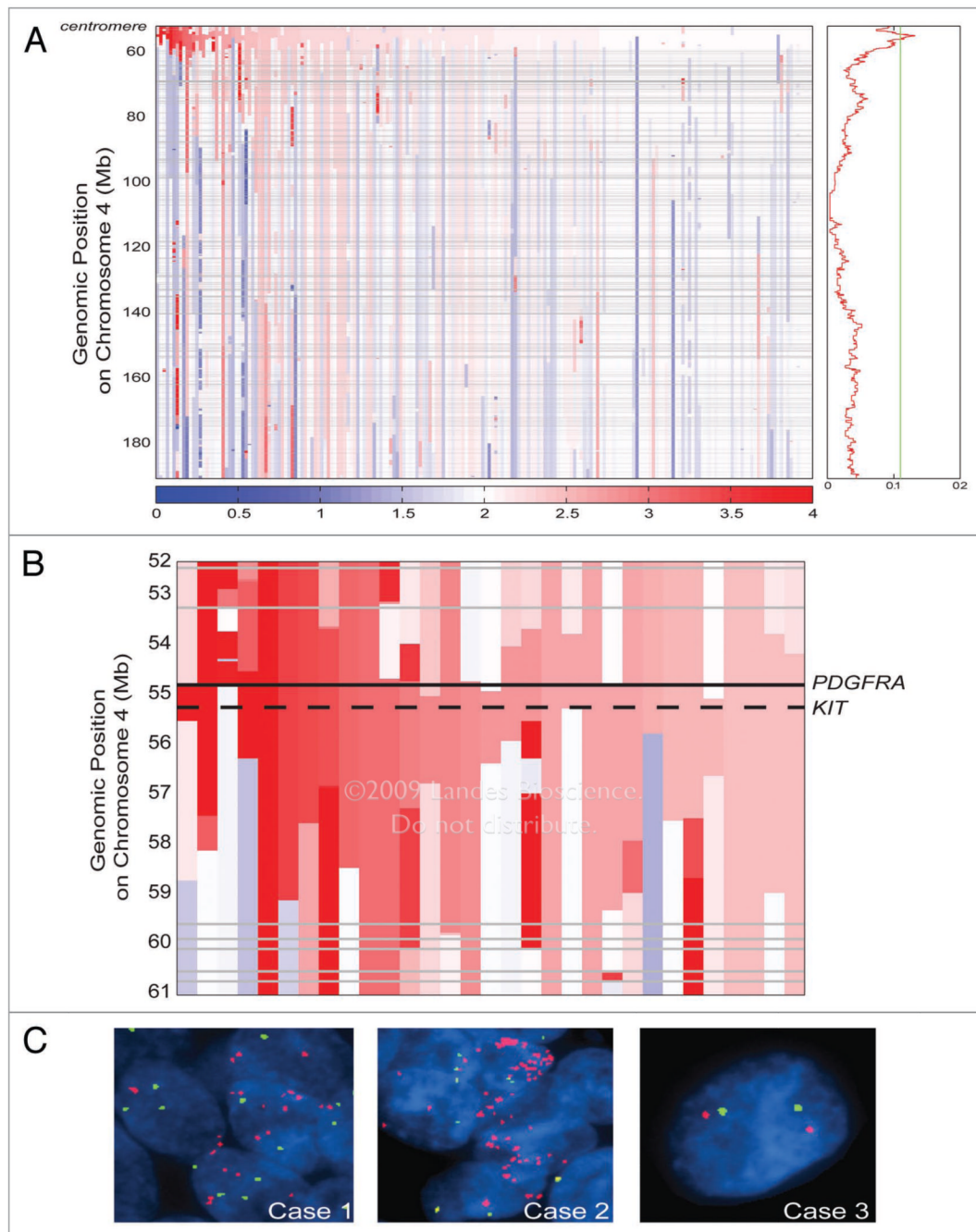


Figure 1.

Recurrent genomic amplifications of *PDGFRA* and *KIT* in NSCLC samples. (A) Smoothed copy number estimates within chromosome arm 4q in top 200 NSCLC samples (columns; ordered by amplification of 4q12). The color scale ranges from blue (deletion) to red (amplification) with estimated copy numbers shown. Grey regions represent the absence of SNP copy number data. Plotted GISTIC G-scores on the right are from all available samples. The green line on the GISTIC plot represents a significance threshold of 0.25 false discovery rate q -value. (B) Magnified view of smoothed copy number estimates from the centromere to 61 Mb on chromosome 4 from 31 NSCLC samples having amplification greater than 2.46 copies (\log_2 ratio of 0.3) at 4q12. Samples are sorted according to the

maximum copy number estimate for *PDGFRA* and *KIT*. Solid and dashed lines indicate positions of *PDGFRA* and *KIT*, respectively. Color scale as in (A). (C) FISH for *PDGFRA* (red) and chromosome 4 reference probe (green) displaying low-level and high-level gain of *PDGFRA* in two different lung squamous cell carcinoma samples, Case 1 and Case 2 respectively. A lung adenocarcinoma sample, Case 3, with no amplification at *PDGFRA* is shown on the right for reference. Nuclei are stained with 4,6-diamidino-2-phenylindole (DAPI; blue).

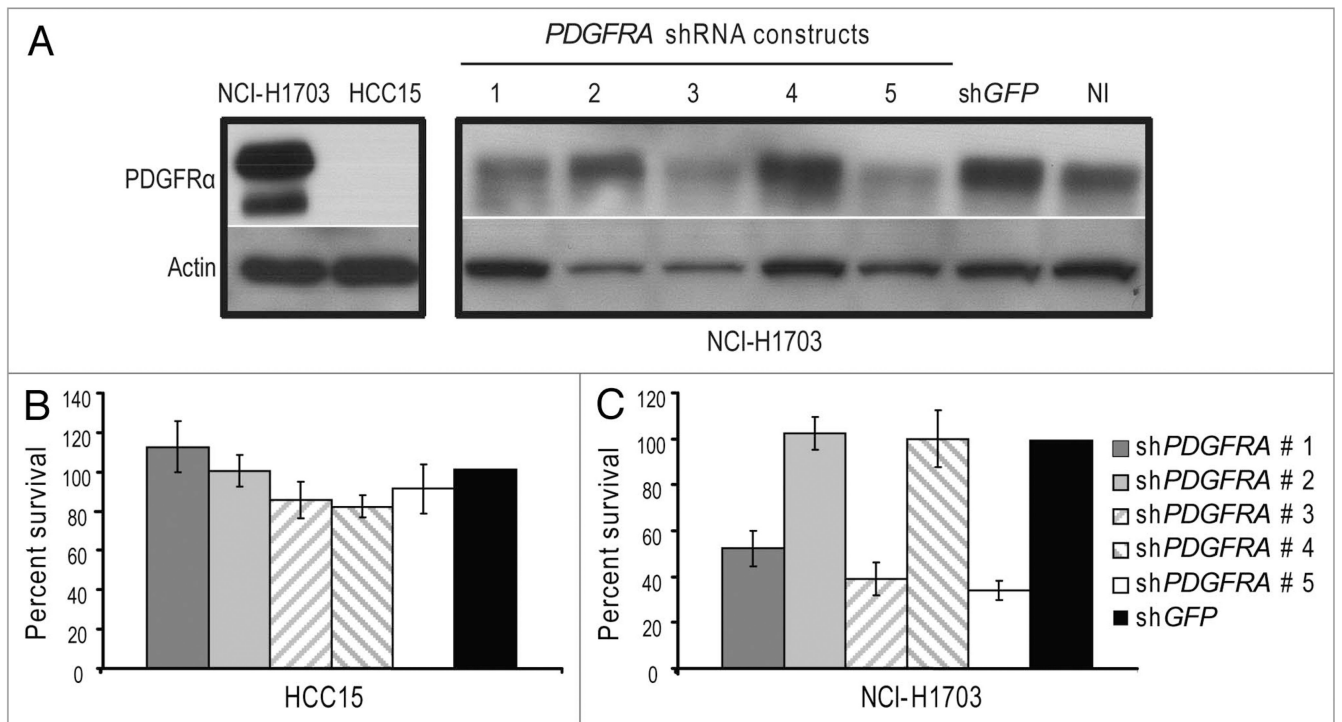


Figure 2.

NCI-H1703 cells are addicted to PDGFR α activity. (A) PDGFR α expression in NCI-H1703 and HCC15 was confirmed by immunoblotting using actin as a loading control (left). shRNA constructs used to knockdown *PDGFR α* expression were packaged into lentivirus and used to infect NCI-H1703 and HCC15 cells. Anti-PDGFR α immunoblot shows that hairpins #1, #3 and #5 efficiently knock down endogenous PDGFR α expression in NCI-H1703 cells. Actin is included as a loading control. NI, no infection. shGFP, control hairpin specific for green fluorescent protein used as a negative control (right). (B and C) Infection with three independent hairpins (#1, #3 and #5) did not inhibit cell survival of HCC15 cells as assessed by WST assay (B) but did inhibit survival of NCI-H1703 cells overexpressing *PDGFR α* (C). All results normalized to survival of cells infected with shGFP.

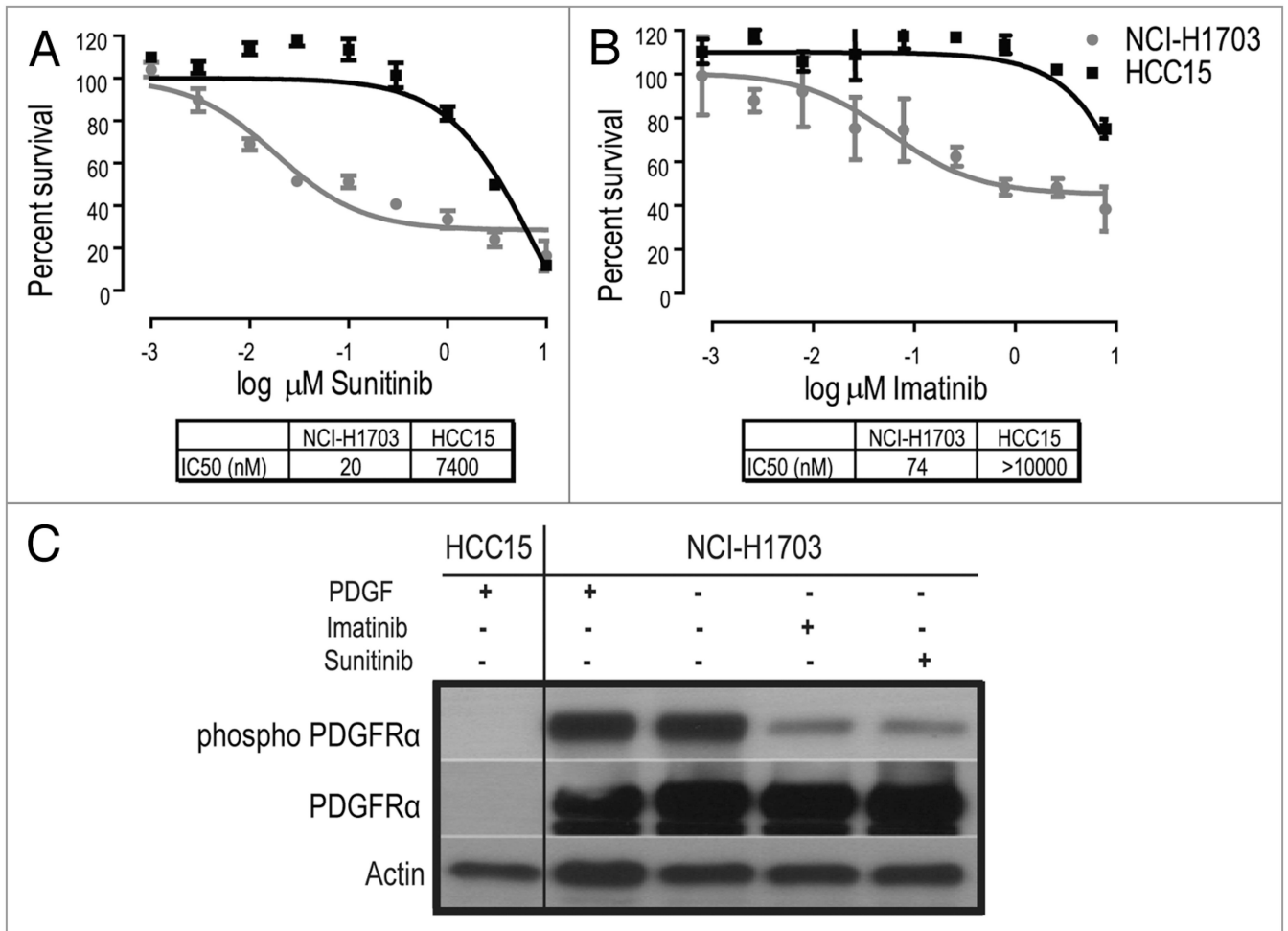


Figure 3.

PDGFR α tyrosine kinase activity is essential in NCI-H1703 cells. (A) PDGFR α is constitutively phosphorylated, with or without PDGF ligand, in NCI-H1703 cells, as compared with HCC15 cells. Stimulation with PDGF was carried out for 20 minutes at 37°C with 100 ng/ml of PDGF. Treatment of these cell lines for 40 minutes with 2 μ M PDGFR kinase inhibitor imatinib and sunitinib inhibits basal phosphorylation, as evidenced by immunoblotting with anti-phospho-PDGFR α (upper). Similar levels of expression of PDGFR α are confirmed by immunoblotting with anti-PDGFR α (middle) using actin as a loading control (lower). (B and C) Treatment with the indicated concentrations of imatinib and sunitinib inhibited survival of NCI-H1703 cells, but not of HCC15 cells, as determined by WST assay performed after 4 days treatment. IC₅₀s are indicated.

Table 1Fluorescent in situ hybridization evaluation of *PDGFRA* in NSCLC samples

Tumor type	Cases evaluated	High-level <i>PDGFRA</i> amplification (CN > 10)	Low-level <i>PDGFRA</i> amplification (CN = 4–10)
Adenocarcinoma	313	12 (3.8%)	9 (2.9%)
SCC	161	14 (8.7%)	3 (1.9%)
Adenosquamous	8	0	0
BAC	2	0	0
Sarcomatoid	1	0	0
NSCLC	13	1 (7.7%)	0
Total	498	27 (5.4%)	12 (2.4%)

Summary of fluorescent in situ hybridization (FISH) from tissue microarrays of NSCLC samples. Number of evaluable cores with high-level gains of *PDGFRA* (>10 copies) or low-level gain (4–10 copies) are shown for each subtype. SCC, squamous cell carcinoma; BAC, bronchio-alveolar carcinoma; NSCLC, non-small cell lung cancer (histological type not specified).